DOI: 10.1002/ange.201301207

Photomechanical Motion

Photoinduced Bending of a Large Single Crystal of a 1,2-Bis(4-pyridyl)ethylene-Based Pyridinium Salt Powered by a [2+2] Cycloaddition**

*Jian-Ke Sun, Wei Li, Cheng Chen, Cai-Xia Ren, Dan-Mei Pan, and Jie Zhang**

Transducing an input energy stimulus into output energy that can power or accomplish mechanical work is a pervasive topic of many scientific disciplines. One of the current issues is to harness the natural and renewable energy sources which have spawned an ever-burgeoning pursuit of novel materials. In the last few years, the research on molecular machines based on the conversion of the molecular geometry change into mechanical motion of macroscale materials has attracted much attention.[1] Although elaborate design and synthesis of various types of supramolecular machines have been reported, to amplify this nanoscale molecular motion in large-scale bulk materials is still a great challenge. Owing to the advantages in remote, temporal and spatial detection, light-induced deformable materials have emerged as excellent candidates for photomechanical applications.[2] Recently, some solid-state photoreactions in highly ordered molecular crystals, such as open-closed ring isomerization,[3] *cis–trans* isomerization[4] and photodimerization[5] have been actively investigated since these reactions are often accompanied by molecular motion, and thus cause morphological changes on the surfaces of single crystals. These achievements show great promise in linking the molecular-scale deformation to macroscale movement of the densely packed crystal. Nevertheless, the reported crystalline materials usually are quite small (on the nanometer or micrometer scale), which may limit their practical applications in real world. Until now, the rational design and assembly of small organic molecules that can generate large macroscopic photomechanical movement still remain a challenge.

The *trans*-1,2-bis(4-pyridyl)ethylene (4,4′-bpe) molecule is a kind of photoactive molecule that can undergo photoinduced [2+2] cycloaddition under a proper packing geometry. Although numerous examples of the solid-state [2+2] cycloaddition have been demonstrated,[6] the exploration of the photomechanical effect on this molecule is quite scarce. The reason is that the restricted motion of this rigidly conjugated small molecule in solid-state reactions limits the microscopic motion to be amplified to macroscopic movement of the bulk materials (especially in a large-scale single crystal). Furthermore, to promote favorable stacking for a cycloaddition reaction, template-induced and coordination-driven self-assembly techniques have been commonly used, which also bring about much more restrictions on the freedom of molecular motion. Herein we report an interesting example of photomechanical motion based on the 4,4′-bpe derivative, 1-(4-carboxybenzyl)-4-[2-(4-pyridyl)-vinyl]-pyridinium chloride (HBCbpeCl; Scheme 1). Compared with the conventional 4,4′-bpe molecule, the incorporation of the carboxybenzyl group onto one end of this molecule affords some advantages that may facilitate the cycloaddition and motion amplification: 1) The addition of the methylene group effectively increases molecular flexibility. 2) A cation–π interaction between the pyridinium ring and the terminal pyridine ring is likely to form and induce a tight molecular stacking in a head-to-tail (HT) fashion,[7] which is beneficial not only in facilitating cycloaddition reactions, but also in ensuring freedom of motion of the substituted side group. 3) The terminal groups of BCbpe can be connected by hydrogen bonds to each other upon the degree of protonation, or form hydrogen bonds with some solvent molecules, which may allow the cohesive force between the molecules to

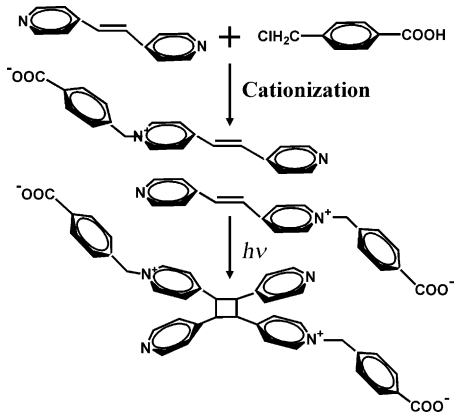

Scheme 1. The cationization of one end of the 4,4′-bpe molecule, a head-to-tail arrangement and photo-cycloaddition.

[*] J. K. Sun, C. Chen, C. X. Ren, D. M. Pan, Prof. J. Zhang
State Key Laboratory of Structural Chemistry
Fujian Institute of Research on the Structure of Matter
CAS Fuzhou, Fujian 350002 (P.R. China)
E-mail: zhangjie@fjirsm.ac.cn
Dr. W. Li
Department of Materials Science and Metallurgy
University of Cambridge, Cambridge CB2 3QZ (UK)

[**] We thank the National Natural Science Foundation of China for financial support (grant numbers 21271173 and 20973171). W. Li is grateful to the University of Cambridge and the European Research Council for providing financial support. Prof. A. K. Cheetham at the University of Cambridge is acknowledged for the great help in measuring the Young's modulus.

Supporting information for this article is available on the WWW under http://dx.doi.org/10.1002/anie.201301207.

be finely tuned by environmental manipulation, and thus render the crystal resistance to mechanical stress to avoid fragmentation. Attractively, the needle-like single crystal **1** (BCbpe·2 H_2O) obtained by self-assembly of the HBCbpeCl compound can undergo remarkable deformation in the centimeter scale upon photoirradiation, and become luminescent on distortion, which gives a big advantage for remote detection of mechanical movements.

Single crystals of **1** were obtained by slow evaporation of the NaOH-neutralized HBCbpeCl in methanol–water mixed solvents within a few days. The typically long needlelike crystals (with the size of 0.5–3.6 cm in length) grew along the *a* axis (for the face indexing see the Supporting Information). Mounted at one end with a tweezers and exposed to a Xe lamp for about 2 s (200 mW cm^{-2}), the needlelike crystal ($1.5 \times 0.08 \times 0.12$ cm^3) undergoes a dramatic deformation that is perpendicular to its longest dimension, bending towards the light source without breaking (Figure S1). To further test the deformation ability of the single crystal, a free-standing single crystal ($0.82 \times 0.07 \times 0.05$ cm^3) on a filter paper is irradiated with a Xe lamp in a controlled manner (Figure 1). The

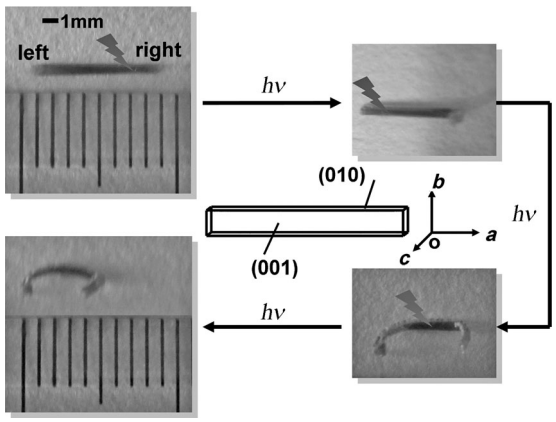

Figure 1. The roll up of a single crystal ($0.82 \times 0.07 \times 0.05$ cm^3) with controlled irradiation. The irradiation light toward the top side of the crystal is perpendicular to its (001) face. The light is focused on different areas in the (001) face at each time.

irradiation light toward the top side of the crystal is perpendicular to the (001) face. Firstly, we focus the irradiation on the top of right side of the crystal. The edge is bent toward the light source. Then we do the same procedure on the top of the left side of the single crystal to roll up another end. Finally, we direct the concentrated light irradiation on the top of the middle of the crystal. The crystal tends to bend around its middle part and shows a tendency to enclose two ends of the crystal. Further effort to fabricate the crystalline ring is failed because of the cracking of the whole crystal, which may be caused by the release of large accumulated structural stress in the crystal lattice. However, the magnitude of bending is unprecedented in deformable crystalline materials especially in view of its large scale (in the centimeter range). It is noted that such deformation is plastic, so that the original shape of the crystals is not restored, even after they have been aged in the dark for a few days.

The observed photomechanical effect should be related to the [2+2] cycloaddition reaction of the BCbpe molecules in **1**. To verify the [2+2] photo-cycloaddition reaction, ^{1}H NMR measurements on the crystals were carried out before and after photoirradiation (Figure S2). It has shown that about 9% of the initial reaction was performed after irradiating a single crystal (3 mg) for 10 s (200 mW cm^{-2}). The small yield of the photoproduct is similar to those observed in the azobenzene or diarylethene derivatives with photomechanical effects,[2–4] which is reasonable since the photoreaction generally occurs on the surface of the crystal because of the high absorbance of the crystals in the UV/Vis region. However, such a proportion is large enough to induce bending of the crystals. ^{1}H NMR spectroscopy revealed that the olefinic groups have reacted to form cyclobutane rings in about 85.4% yield after photoirradiation for 48 h. To further demonstrate the photodimerization reaction, the powdered crystalline **1** was irradiated for a prolonged time, and then dissolved in mixed water–methanol solvents. X-ray single-crystal diffraction analysis on the recrystallized yellow compound definitely confirmed the formation of a HT-type σ-dimer after photoirradiation (Figures S3 and S4).

For a [2+2] cycloaddition reaction to occur in the solid state, the adjacent reactive double bonds should be packed in parallel with a distance less than 4.2 Å. X-ray crystallographic analysis reveals that **1** crystallizes in the monoclinic space group $P2_1/c$. The bpe moieties stack in columns along the crystallographic *a* axis and are oriented in a HT manner with alternate distances of 3.60 and 3.65 Å between the reactive olefin carbon atoms, and the distances of 3.50 and 3.74 Å between adjacent pyridine and pyridinium rings, suggesting a significant contribution and role of the cation–π interaction in controlling the molecular packing (Figure 2 and Figure S5 in the Supporting Information). The corresponding geometrical parameters θ_1, θ_2, θ_3, D_1, and D_2[8] (see Table S1 in the Supporting Information) are in accordance with the high photoactivity of the crystal **1**. The carboxybenzyl group substituted on a nitrogen atom of the bpe molecule is twisted by 88.94° from the bpe plane, hanging alternately on the two sides of the bpe column with larger interval. Interestingly, two carboxylate oxygen atoms from different columns, together with four symmetry-related water molecules, form a hydrogen-bonded six-membered ringlike buckle (O···O distances of 2.77–2.79 Å), which associates with each other through weak hydrogen-bonding interactions (the O···O distance: 2.85 Å) and holds the 1D column units into 2D undulating layer. These layers are stacked in a -ABAB- pattern with the six-membered ring unit and bpe moiety staggered relative to each other.

Although numerous solid-state [2+2] cycloaddition reactions based on 4,4′-bpe derivatives have been demonstrated, no photomechanical effect has been observed for their molecular assemblies. Besides a disadvantage caused by the intrinsic rigidity of the 4,4′-bpe molecule, the prevalent strategies to align the olefinic bonds in optimal orientation for cycloaddition, including template or coordination-driven self-assembly, also restrict the mobility of molecules to some extent. From the structurally well-characterized examples that undergo photoinduced cycloaddition in the solid state,[9]

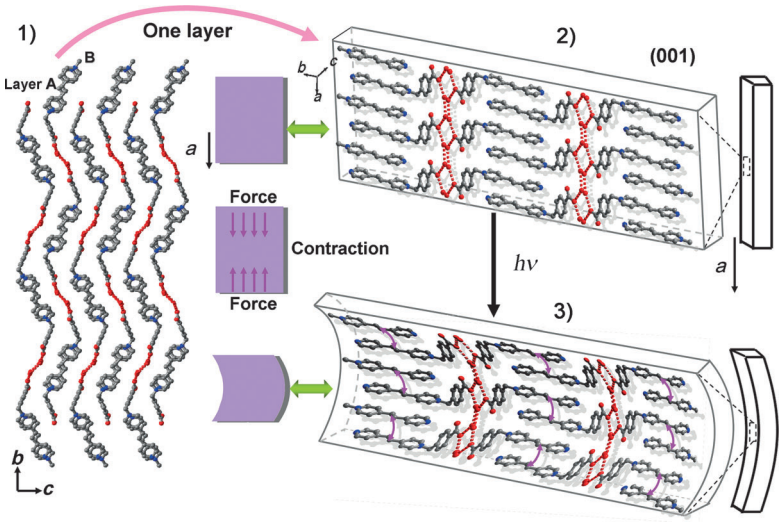

Figure 2. Illustrations of the bending direction of crystal **1** and related crystal structure. 1) The 2D supramolecular layers are stacked in an -ABAB- manner. 2) The molecular arrangement in the (001) face. 3) The [2+2] cycloaddition induces the contraction of the planes parallel to the (001) face, leading to the bending perpendicular to the *a* axis of the crystal. All hydrogen atoms in the structures were omitted for clarity.

it can be found that the 4,4′-bpe molecules are anchored to the molecular skeleton by coordination or hydrogen-bonding interactions, their molecular movements are difficult to be propagated out because of the restriction of a rigid geometry. By engineering 4,4′-bpe molecule to meet the condition for forming cation–π interactions, the derivative BCbpe molecules are directed into a parallel head-to-tail close arrangement suitable for cycloaddition without the assistance of a template, and stacked in infinite columns that are favorable for transferring nanoscale cycloaddition motion along a specific direction. It should be noted that the photoreactivity of the bpe-based derivatives arranged in an infinite parallel array congenial for a cycloaddition reaction is still less explored and no deformation phenomenon of crystals has been reported.[6a,10] Compared with these molecular assemblies, the present compound possesses additional structure advantages responsible for its macroscopically photomechanical deformation: 1) The introduction of the carboxybenzyl group increases the molecular flexibility because of the freely rotating CH_2 junction, allowing large conformational change to occur in response to environmental stress. 2) The adjacent BCbpe molecules are joined together by hydrogen bonds between the carboxylate oxygen atoms and water molecules. Each junction is present as six-membered ringlike structure and associates with each other through weak hydrogen-bonding interactions in a parallelogramlike linkage pattern. By virtue of these deformable hexagon and parallelogram structures, the hydrogen-bonded molecular layer possesses a high binding strength and flexibility to withstand greater tensile strain. 3) The BCbpe molecules and flexible joints in adjacent layers are arranged in a staggered pattern. This arrangement is expected to increase the deformation tolerance of the molecular aggregates to mechanical stress. By analyzing the relationship between microscopic packing and macroscopic crystal growth directions (Figures S6–S8), we deduce that the photo-cycloaddition generates a contraction force, which is accumulated and amplified through the infinite π-stacked parallel column, resulting in the anisotropic contraction of the (001) plane. Since the high absorbance of the dense crystal hinders a deeper penetration of light, the photoreaction only occurs in the surface region of the crystal. The difference in the degree of contraction leads to the bending of the crystal toward the irradiated light (Figure 2). This bending process is reminiscent of the bilayer cantilever effect. The cantilever becomes curved by a bending moment caused by the mismatch of the stress in each layer.[11] The crystal presented here may be also considered to be composed of reacted and unreacted layers with different local stresses, which induce the bending of the crystal. The molecular deformation induced by [2+2] cycloaddition can also be reflected in the microscopic surface of the single crystal. We use the real-time AFM images to record the surface morphological changes after photoirradiation. The original surface of the crystal is relatively smooth with an average roughness of 1.1 nm. Upon irradiation, the surface of initial crystal becomes rugged and the roughness has increased gradually to 2.6 nm then to 6.7 nm with increasing irradiation time, accompanied by the appearance of ridge-like structures (Figures S9 and S10).

To reveal the mechanical strength of the single-crystal materials, the Young's modulus is measured via nanoindentation which is established as an effective method to assess the mechanical response of solids with high precision. Nanoindentation measurements are performed using a sharp Berkovich tip (tip radius ≈100 nm) in a continuous stiffness measurement (CSM) mode. The indenter axis is aligned normal to the artificially polished (011) and $(1\bar{1}0)$ orientated facets of single crystal **1**. Representative *P*–*h* curves obtained on both facets are shown in Figure 3. The loading part of both facets is smooth, indicating that the plastic deformation, which occurs underneath the Berkovich tip during indentation, is relatively homogeneous in nature. The average values of elastic modulus (E) and hardness (H) normal to (011) and $(1\bar{1}0)$ of **1**, extracted from the *P*–*h* curves, are calculated over depths of 200–1000 nm in order to minimize the imperfection of the Berkovich tip.[12] Although the loading during indentation is not perfectly uniaxial and the stress field generated underneath the indenter is nonuniform, indentation can be used to probe the mechanical properties of single crystals since the measured modulus is strongly dependent on the elastic response along the indenter axis and is weakly affected by the transverse directions.[13] The average elastic moduli normal to the orthogonal facets were found to be $E_{(011)} = 10.284 \pm 0.204$ GPa and $E_{(1\bar{1}0)} = 9.670 \pm 0.371$ GPa, which are much larger than those of typical polymeric materials (ca. 1 GPa) and are comparable to a handful of organic crystals (8.5–15 GPa).[3b,13a,b,14] The high Young's modulus and large deformation of **1** indicate that the photocycloaddition reac-

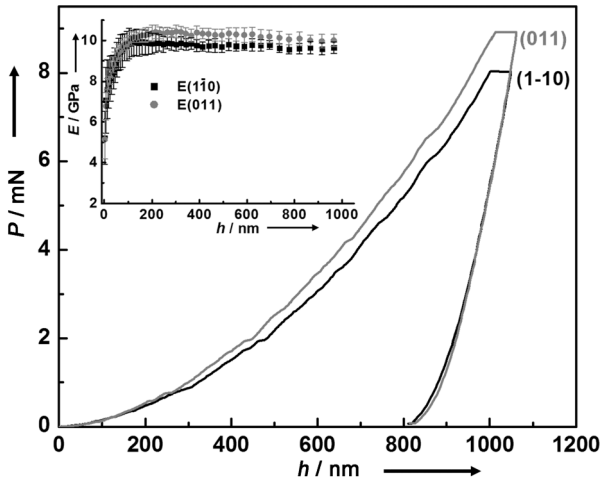

Figure 3. Representative *P* (Load)–*h* (*h* = indentation depth) curves for **1** with the (1$\bar{1}$0) and (011) orientated facets measured by a Berkovich tip. Inset: elastic moduli E of **1** as a function of the indentation depth, wherein each error bar represents the standard deviation from 20 indents.

tion could generate a strong force to exceed the elastic threshold of the single crystal and carry out large mechanical work.

The photoirradiation not only generates a photomechanical effect, but also induces the luminescence switching. The crystalline sample is nonluminous in the initial state but shows highly visual red luminescence emission under UV light ($\lambda =$ 365 nm) after several minutes of irradiation (Figure 4 and Figure S11). Spectral measurements reveal that the photoirradiated sample exhibits a wavelength-dependent dual emission behavior. Upon excitation at 385 nm, two emission peaks centered at 458 and 647 nm can be detected. With increasing the excitation wavelength, the spectra are dominated by the emission in the long-wavelength region. In

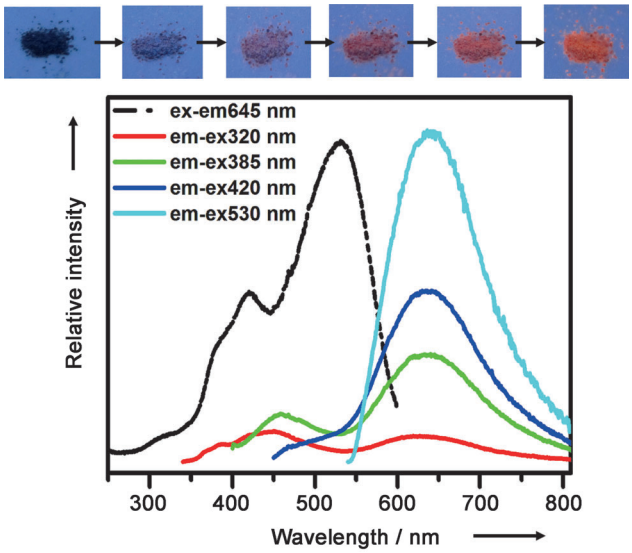

Figure 4. Top panel: Fluorescence image of powdered crystal **1** upon UV irradiation, $\lambda_{ex} = 365$ nm. Bottom panel: The excitation (black line) and emission (colored lines) spectra of irradiated sample **1**.

contrast with usual on–off luminescence photoswitching systems, the examples involving the photoswitching from nonfluorescent to fluorescent state are scarce,[15] although great interest has been aroused due to their high contrast ratio (10^2) and powerful applications in super-resolution fluorescence imaging that requires initial dark background.[16] In particular, such distortion-promoted luminescence process is essential for remote detection of photomechanical work because of its high visual contrast. To explore the emission mechanism of this process, the photoluminescence behavior of the BCbpe molecule in solution is studied. Remarkably, the emission profile in methanol is quite similar to that of the photoirradiated sample, and exhibits the wavelength dependent emission behaviors (Figure S12). Moreover, the pure σ-dimer is almost nonluminescent under the same condition. These results reveal that the photoluminescence switching occurring simultaneously during the deformation process should originate from the liberated BCbpe monomers. The excitation wavelength-dependent emission profiles from dual to single emission behavior are attributed to the enhancement of intramolecular charge transfer (ICT) emission as it is consistent with an observation on the cationic stilbazolium derivatives incorporating both donor and acceptor in solution state,[17] and it is further demonstrated by solvent polarity-dependent emission (Figure S13). We speculate that the [2+2] cycloaddition may induce the changes in molecular conformation or packing pattern in the crystals and thus weaken the intermolecular interaction of partial BCbpe molecules, leading to a fluorescence change from quenching to emitting state.

In summary, we have successfully realized photodriven mechanical movement of crystalline materials on the macroscopic scale based on a derivate of the 4,4′-bpe molecule. The deformation scale of the single crystal is by far the largest among the reported photomechanical crystalline materials. Attractively, the deformation process is accompanied with high fluorescence visual contrast, which makes it an excellent candidate for remote detection of photomechanical work. The present work may provide some clues for developing macroscopically photomechanical crystalline materials based on small organic molecules.

Received: February 11, 2013
Revised: April 19, 2013
Published online: May 21, 2013

Keywords: cycloaddition · photomechanical properties · pyridinium salts · single crystals

[1] a) M. M. Boyle, R. A. Smaldone, A. C. Whalley, M. W. Ambrogio, Y. Y. Botros, J. F. Stoddart, *Chem. Sci.* **2011**, *2*, 204; b) W. R. Browne, B. L. Feringa, *Nat. Nanotechnol.* **2006**, *1*, 25; c) K. M. Lee, D. H. Wang, H. Koerner, R. A. Vaia, L. S. Tan, T. J. White, *Angew. Chem.* **2012**, *124*, 4193; *Angew. Chem. Int. Ed.* **2012**, *51*, 4117.

[2] a) H. Koerner, T. J. White, N. V. Tabiryan, T. J. Bunning, R. A. Vaia, *Mater. Today* **2008**, *11*, 34; b) D. Bléger, Z. L. Yu, S. Hecht, *Chem. Commun.* **2011**, *47*, 12260; c) M. Yamada, M. Kondo, J. Mamiya, Y. Yu, M. Kinoshita, C. J. Barrett, T. Ikeda, *Angew. Chem.* **2008**, *120*, 5064; *Angew. Chem. Int. Ed.* **2008**, *47*, 4986.

[3] a) S. Kobatake, S. Takami, H. Muto, T. Ishikawa, M. Irie, *Nature* **2007**, *446*, 778; b) M. Morimoto, M. Irie, *J. Am. Chem. Soc.* **2010**, *132*, 14172.
[4] H. Koshima, N. Ojima, H. Uchimoto, *J. Am. Chem. Soc.* **2009**, *131*, 6890.
[5] a) L. Y. Zhu, R. O. Al-Kaysi, C. J. Bardeen, *J. Am. Chem. Soc.* **2011**, *133*, 12569; b) P. Naumov, J. Kowalik, K. M. Solntsev, A. Baldridge, J. S. Moon, C. Kranz, L. M. Tolbert, *J. Am. Chem. Soc.* **2010**, *132*, 5845.
[6] a) M. Nagarathinam, A. M. P. Peedikakkal, J. J. Vittal, *Chem. Commun.* **2008**, 5277; b) G. K. Kole, G. K. Tan, J. J. Vittal, *J. Org. Chem.* **2011**, *76*, 7860; c) L. R. MacGillivray, G. S. Papaefstathiou, T. Friščić, T. D. Hamilton, D. K. Bučar, Q. L. Chu, D. B. Varshney, I. G. Georgiev, *Acc. Chem. Res.* **2008**, *41*, 280.
[7] S. Yamada, Y. Tokugawa, *J. Am. Chem. Soc.* **2009**, *131*, 2098.
[8] V. Ramamurthy, K. Venkatesan, *Chem. Rev.* **1987**, *87*, 433.
[9] a) Y. C. Ou, W. T. Liu, J. Y. Li, G. G. Zhang, J. Wang, M. L. Tong, *Chem. Commun.* **2011**, *47*, 9384; b) G. S. Papaefstathiou, Z. M. Zhong, L. Geng, L. R. MacGillivray, *J. Am. Chem. Soc.* **2004**, *126*, 9158; c) L. R. MacGillivray, J. L. Reid, J. A. Ripmeester, *J. Am. Chem. Soc.* **2000**, *122*, 7817.
[10] B. R. Bhogala, B. Captain, A. Parthasarathy, V. Ramamurthy, *J. Am. Chem. Soc.* **2010**, *132*, 13434.
[11] J. N. Kuo, G. B. Lee, W. F. Pan, H. H. Lee, *Jpn. J. Appl. Phys.* **2005**, *44*, 3180.
[12] J. Gong, H. Miao, Z. Peng, *Mater. Lett.* **2004**, *58*, 1349.
[13] a) S. Varughese, M. S. R. N. Kiran, K. A. Solanko, A. D. Bond, U. Ramamurty, G. R. Desiraju, *Chem. Sci.* **2011**, *2*, 2236; b) M. S. R. N. Kiran, S. Varughese, C. M. Reddy, U. Ramamurty, G. R. Desiraju, *Cryst. Growth Des.* **2010**, *10*, 4650; c) J. C. Tan, A. K. Cheetham, *Chem. Soc. Rev.* **2011**, *40*, 1059.
[14] a) C. M. Reddy, R. C. Gundakaram, S. Basavoju, M. T. Kirchner, K. A. Padmanabhan, G. R. Desiraju, *Chem. Commun.* **2005**, 3945; b) F. Terao, M. Morimoto, M. Irie, *Angew. Chem.* **2012**, *124*, 925; *Angew. Chem. Int. Ed.* **2012**, *51*, 901.
[15] a) K. Uno, H. Niikura, M. Morimoto, Y. Ishibashi, H. Miyasaka, M. Irie, *J. Am. Chem. Soc.* **2011**, *133*, 13558; b) J. W. Chung, Y. You, H. S. Huh, B.-K. An, S.-J. Yoon, S. H. Kim, S. W. Lee, S. Y. Park, *J. Am. Chem. Soc.* **2009**, *131*, 8163.
[16] a) E. Betzig, G. H. Patterson, R. Sougrat, O. W. Lindwasser, S. Olenych, J. S. Bonifacino, M. W. Davidson, J. Lippincott-Schwartz, H. F. Hess, *Science* **2006**, *313*, 1642; b) M. J. Rust, M. Bates, X. W. Zhuang, *Nat. Methods* **2006**, *3*, 793.
[17] a) B. Wandelt, P. Turkewitsch, B. R. Stranix, G. D. Darling, *J. Chem. Soc. Faraday Trans.* **1995**, *91*, 4199; b) X. H. Jin, J. Wang, J. K. Sun, H. X. Zhang, J. Zhang, *Angew. Chem.* **2011**, *123*, 1181; *Angew. Chem. Int. Ed.* **2011**, *50*, 1149; c) J. K. Sun, X. H. Jin, L. X. Cai, J. Zhang, *J. Mater. Chem.* **2011**, *21*, 17667.

